

DROCC: Deep Robust One-Class Classification

Sachin Goyal¹ Aditi Raghunathan² Moksh Jain³ Harsha Vardhan Simhadri¹ Prateek Jain¹

Abstract

Classical approaches for one-class problems such as one-class SVM (Schölkopf et al., 1999) and isolation forest (Liu et al., 2008) require careful feature engineering when applied to structured domains like images. To alleviate this concern, state-of-the-art methods like DeepSVDD (Ruff et al., 2018) consider the natural alternative of minimizing a classical one-class loss applied to the *learned* final layer representations. However, such an approach suffers from the fundamental drawback that a representation that simply collapses all the inputs minimizes the one class loss; heuristics to mitigate collapsed representations provide limited benefits. In this work, we propose Deep Robust One Class Classification (DROCC) method that is robust to such a collapse by training the network to distinguish the training points from their perturbations, generated adversarially. DROCC is motivated by the assumption that the interesting class lies on a locally linear low dimensional manifold. Empirical evaluation demonstrates DROCC’s effectiveness on two different one-class problem settings and on a range of real-world datasets across different domains—images (CIFAR and ImageNet), audio and time-series, offering up to 20% increase in accuracy over the state-of-the-art in anomaly detection.

1. Introduction

Several modern learning applications require strong “one-class” classifiers that are accurate discriminators for a special, well-sampled class. Anomaly detection is one of the most well-known problems in this domain where the data is predominantly from only one class (the normal class) and the goal is to identify if a point belongs to the normal class or the abnormal class. Low false positive rate constrained One-class Classification (LFOC) is another important prob-

lem in this domain that we will formally introduce later, but has several applications like in the audio/visual wakeword domain where the goal is to ensure high recall of wakeword while ensuring small false positive rate (FPR) against arbitrary distribution over negatives.

Anomaly detection in particular has been subject of a vast amount of research works. Classical approaches for anomaly detection model the provided “normal” data using a learned function and label a point as anomalous if it’s agreement with the learned function is small. OC-SVM (Schölkopf et al., 1999) uses minimum-enclosing ball, isolation forest (Liu et al., 2008) uses axis-aligned cuts and PCA based approaches (Lakhina et al., 2004) use low-dimensional subspace to model the data.

These techniques are well-suited for featurized data, however for more complex data structures like images/speech, the same techniques struggle significantly as their function classes are ill-suited to model them. A natural approach is to apply the above mentioned techniques over the learned representations using the datatype specific deep neural networks (DNNs) architectures, e.g., using CNNs for images (Ruff et al., 2018). However, since the representation learning is dictated by the data-modeling layer, it leads to *representation collapse*. That is, it would naturally learn trivial representations that map all the points to a single point (like origin) as that will have the best fit w.r.t. the data-model class (example by a minimum enclosing ball or subspace).

Recently, several techniques have been proposed to avoid such representation collapse. These methods either use some heuristics like zero-bias (Ruff et al., 2018) which are still not robust as the global optima remains the collapsed representation or assume more information about the problem and the datatype. For example, (Golan & El-Yaniv, 2018; Bergman & Hoshen, 2020) require a set of transformations to learn effective representations, while (Hendrycks et al., 2019a) requires access to certain out-of-sample anomalies.

In this paper, we propose a novel *Deep Robust One-Class Classification* (DROCC) method for anomaly detection that can also be extended to other one-class classification problems. In particular, our method is motivated by the key observation that typically the normal class data tend to lie on a well-sampled low-dimensional manifold — which has

¹Microsoft Research, India ²Stanford University, USA
³National Institute of Technology, Karnataka, India. Correspondence to: Prateek Jain <prajain@microsoft.com>.

been believed to be true for the most complicated data domains as well, like vision, speech and natural language (Pless & Souvenir, 2009). As manifolds resemble Euclidean space locally, we can use the standard L_2 distance function to compare points in a small ball around each training point. That is, we can cast the problem as a classification problem where the training points belong to the “normal” class while any point *outside* the union of small L_2 balls around each training point are treated as “abnormal”. Note that while (Golan & El-Yaniv, 2018; Bergman & Hoshen, 2020) also cast the problem as a classification problem, our formulation applies to the general anomaly detection problem, it does not require additional information about transformations and in fact it can be used as a complementary technique.

The resulting problem formulation is closely related to adversarial training and it motivates our stochastic gradient descent-ascent based training algorithm. Intuitively, the gradient ascent phase adds more and more negative (abnormal) points to our training set and the gradient descent algorithm learns a representation of the points and a classifier that separates normal points from the abnormal points.

Next, we study a critical problem of similar flavor that we refer to as Low FPR One-class Classification (LFOC), which, despite being encountered in many real-world scenarios, has not been rigorously studied in the literature (to the best of our knowledge). Given a well-sampled positive (or interesting) class and a few samples from the negative (or uninteresting) class, the goal of LFOC is to design a binary classification method that has low FPR against arbitrary distribution of negatives (or uninteresting class) while ensuring accurate prediction accuracy for in-distribution positives. For example, audio wakeword detection is a popular problem in this domain, where the goal is to identify certain wakeword like “Marvin” in given speech stream. For training, we can collect some amount of negative data where the keyword “Marvin” has not been uttered. However, standard representation learning algorithms tend to focus only on some easy to identify substring of “Marvin” like say “Mar”, which is far from the negatives. This leads to a large number of out-of-distribution (OOD) false positives as the classifier will identify words like “Marvelous” or “Martha” as the “Marvin” wakeword. Typical methods in the literature suggest collection and addition of such false positives to the training data to make it more robust, but that is an expensive and oftentimes infeasible process.

In contrast, we can extend our DROCC method to the LFOC problem. Our novel method DROCC – LF uses a similar low-dimensional manifold assumption for the “positive” class data, but it also uses the provided negative data to learn a better representation. Additionally, representation map from the additional data allows us to identify certain coordinates/features of the data points that are “noisy” which

in turn helps us use a more robust locally *elliptical* distance function than the locally Euclidean distance function (which requires manifold to be sampled tightly).

Empirical evaluation on both the above mentioned problems suggests that our technique is able to model the interesting class more robustly than the baselines and can provide significantly more accurate solution. For example, when applied to the anomaly detection task on benchmark CIFAR-10 dataset, our method can be up to 20% more accurate than the baseline methods like DeepSVDD and Autoencoder. Similarly, for time-series problems like anomaly detection with ECG signals, our method can be 4-5% more accurate than DeepSVDD and 20% more accurate than Autoencoder. Finally, for LFOC problem, our method can be up to 10% more accurate than the standard baselines.

In summary, the paper makes the following contributions:

- We propose DROCC method that uses low-dimensional manifold assumption with standard adversarial training style formulation to obtain an accurate classification based solution for the anomaly detection problem.
- We introduce the LFOC problem where the goal is to design a method with low FPR despite arbitrary test distribution over negatives. Further, we extend DROCC method to address the problem by using both the provided labeled training data along with the adversarially generated negative points.
- Finally, we conduct experiments with image, audio as well as time-series data and demonstrate effectiveness of our methods when compared to the standard baselines.

2. Related Work

Anomaly Detection: Anomaly Detection (AD) has been extensively studied owing to its wide applicability (Chandola et al., 2009; Goldstein & Uchida, 2016). (Schölkopf et al., 1999) presented an unsupervised support vector based algorithm and (Tax & Duin, 2004) provided an alternative formulation which minimizes the volume of the hypersphere enclosing the training points projected in the kernel space. Isolation forest (Liu et al., 2008) is one of the most successful technique for AD, which constructs multiple trees from the given data and the anomalous samples are hypothesized to be isolated much closer to the root than normal samples. PCA based anomaly detection methods (Lakhina et al., 2004) assume that the normal points lie on a low-dimensional linear subspace and anomalies lie far from that subspace. Recent analysis by Gu et al. (2019) has also demonstrated the effectiveness of nearest-neighbour methods for unsupervised anomaly detection.

Deep Anomaly Detection: The above mentioned methods require featurized data points which are difficult to design. Deep AD methods attempt to learn the features or represen-

tation while also modeling the normal data points. Deep Autoencoders have been studied extensively in this domain as they capture the underlying data distribution in an unsupervised fashion and thus are a good fit for AD (Malhotra et al., 2016; Sakurada & Yairi, 2014). ConAD (Nguyen et al., 2019) builds upon these techniques and proposes multi-head decoder to ensure lower reconstruction error and good representation learning. As we argued in next section, autoencoder based techniques attempt to solve a harder problem than anomaly detection, and hence are relatively inaccurate on noisy datasets (see Table 1 and Section 3).

Deep SVDD (Ruff et al., 2018) introduced the first fully deep one-class classification objective for anomaly detection. DeepSVDD involves jointly training a deep neural network while optimizing a data-enclosing hypersphere in output space to extract common factors of variation from the data. DeepSVDD, however, is susceptible to collapsing to representations that simply minimize the one-class loss. DROCC is robust to such collapse since it learns representations to classify training points from their perturbations.

(Golan & El-Yaniv, 2018; Hendrycks et al., 2019b) proposed discriminative approaches that leverage transformations of normal image to learn representations for anomaly detection. Recently, (Bergman & Hoshen, 2020) generalized the idea to tabular data by using handcrafted affine transforms. One drawback of such techniques is that they require additional information about the domain like permissible transformations of the data which can be difficult to design. For example, for time-series data, designing such transformations is challenging. Further, even for image data, standard transformations like rotation/flipping might not be suitable in certain applications. For example, an anomaly detector running on CCTV camera should alert if a person appears horizontal or upside down. In contrast, the low-dimensional manifold assumption that motivates DROCC is general and extends to several data modes like images, speech, etc.

Recently, several outlier-exposure based methods have also been proposed for anomaly detection (Hendrycks et al., 2019a). These methods requires access to certain OOD samples to make the anomaly detection methods robust. (Ruff et al., 2020) explores orthogonal direction where a small set of labeled anomalous examples are available. They propose a generalized version of DeepSVDD that takes into account the set of labeled examples. In contrast, we study the anomaly detection problem in the general unsupervised learning setting and do not assume any side-information.

Finally, LFOC problem seems similar to the out-of-distribution (OOD) detection problem (Hendrycks & Gimpel, 2016; Hendrycks et al., 2019a) as LFOC’s goal is also to ensure good performance over out-of-distribution *negatives*. However, the goal and the setting of the two problems is significantly different. OOD detection methods have addi-

tional OOD samples that are used to detect if a point is OOD while in LFOC we are only provided in-sample datapoints. Furthermore, OOD detector will fire even if certain positive was out-of-distribution while LFOC is ambivalent to OOD samples for positives, it only needs to be robust w.r.t. OOD samples from the negative class.

3. Anomaly Detection

Let $\mathcal{S} \subseteq \mathbb{R}^d$ denote the set of *normal*, i.e., non-anomalous data points. A point $x \in \mathbb{R}^d$ is *anomalous* or *abnormal* if $x \notin \mathcal{S}$. Suppose we are given n samples $D = [x_i]_{i=1}^n \in \mathbb{R}^d$ as training data, where $D_S = \{i, s.t. x_i \in \mathcal{S}\}$ is the set of normal points sampled by the training data and let $|D_S| \geq (1 - \nu)|S|$ i.e. $\nu \ll 1$ fraction of points in D are anomalies. Then, the goal in *unsupervised* anomaly detection (AD) is to learn a function $f_\theta : \mathbb{R}^d \mapsto \{-1, 1\}$ such $f(x) = 1$ when x is normal and $f(x) = -1$ when x is an anomaly. The anomaly detector is parameterized by some parameters θ .

3.1. Background

The problem of anomaly detection has been widely studied and a number of different approaches have been proposed. Below, we outline the key idea behind two main approaches and discuss their challenges which also serves as a motivation for our DROCC method. See Section 2 for a survey of other relevant anomaly detection methods.

Minimum Enclosing Ball and related methods. First family of approaches is the popular methods of One-class SVM (OC-SVM), Support Vector Data Description (SVDD) and their variants (Schölkopf et al., 1999; Tax & Duin, 2004). Broadly, this class of methods hypothesizes that all normal points lie in a small ball, reducing the AD problem to that of finding a ball of minimum radius that encloses all the training points, i.e., estimate

center μ and radius R such that (ignoring slack variables and other nuances):

$$\theta^{\text{svdd}} \stackrel{\text{def}}{=} [\mu, R] = \min R \text{ s.t. } \|\phi(x_i) - \mu\|_2 \leq R, \forall i \quad (1)$$

where ϕ is some feature map induced by a suitable RKHS. Performance of the above approach depends on the “quality” of feature representation ϕ and in general, requires careful feature engineering for the given task.

To alleviate this issue, Deep-SVDD (Ruff et al., 2018) uses a deep network to parameterize and learn the feature representation ϕ , and then applies the same objective as in 1 to the last layer of the network. However, the method faces a significant challenge which is that neural network’s representation can collapse, i.e., it can learn $\phi(x_i) = \phi(x_j)$ for all $x_i, x_j \in \mathbb{R}^d$. For example, if the initialization was such that every weight is 0, then for the above identity map representation, the final objective function in (1) would be

the globally optimal with $R = 0$. In order to prevent such a collapse, Deep-SVDD uses careful heuristics such as random initialization with large enough variance, but they only provide limited success and can be highly unstable in some cases (discussed in Section 5).

Autoencoder-decoder based anomaly detection. Another approach to anomaly detection is based on using an autoencoder-decoder setup. The idea is to learn a condensed representation using an *encoding* function that captures the key features of the data. The *decoder* then aims to reconstruct the input from the encoded representation. Both the encoder and the decoder are learnt jointly to minimize the reconstruction error. An anomaly is determined to be an input that has high reconstruction error. Intuitively, if the \mathcal{S} lies on a low dimensional manifold/subspace, then that can be accurately captured by the autoencoder. Hence, points with small reconstruction error are normal points and with high error are anomalous. Note that this technique avoids the representation collapse problem but needs to restrict the bottleneck layer’s dimension, else the solution can degenerate to an identity map. Furthermore, the method is trying to reconstruct *entire* point from it’s low-dimensional representation. On the other hand, if a method can identify if a given point lies *somewhere* on the manifold, that itself would be enough to determine if it is a normal point.

In summary, the issue with Deep-SVDD is that it lacks any hypothesis class for the points, hence it cannot avoid collapsed representation. In contrast, autoencoder based approach models the data using low-dimensional manifold but attempts to solve a harder problem of finding it’s embedding in low-dimensional space instead of just identifying if the point belongs to the manifold. Our method is motivated by the above mentioned shortcomings of the two approaches, and uses manifold to model the normal data but uses a classification based formulation to discriminate between points on the manifold and off the manifold.

3.2. Deep Robust One Class Classification

We now present our approach to unsupervised anomaly detection that we call Deep Robust One Class Classification (DROCC). Our approach is based on the following hypothesis: *The set of normal points \mathcal{S} lies on a low dimensional locally linear manifold that is well-sampled.* In other words, outside a small radius around a normal training point, most points are anomalous. Furthermore, as manifolds are locally Euclidean, we can use the standard L_2 distance function to compare the points in a small neighborhood. Figure 1a shows a 1-d manifold and intuitively, why in neighborhood of x_i we can use L_2 distances.

Formally, for a DNN architecture $f_\theta : \mathbb{R}^d \rightarrow \mathbb{R}$ parameterized by θ , and a small radius $r > 0$, DROCC sets θ^{drocc} as the optimal solution to the following problem:

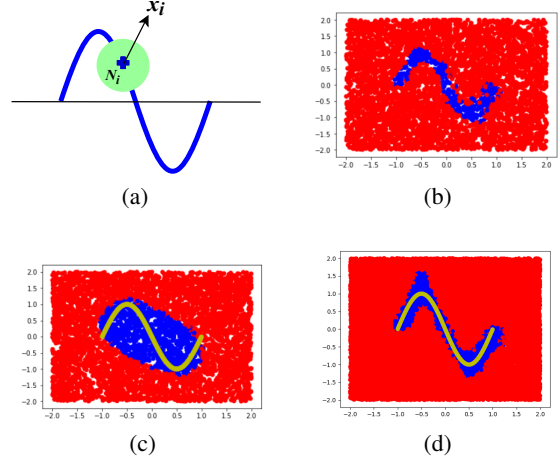


Figure 1. (a) Low dimensional manifold that captures the *normal* data, and a Euclidean ball centered at x_i , (b) Decision boundary of DROCC using only positive points lying on the manifold in plot (a). Blue represents points classified as normal and red points are classified as abnormal. (c) Decision boundary of DROCC when applied to noisy manifold data (Section 5.2). (d) DROCC – LF’s decision boundary for the noisy manifold data which is nearly optimal while DROCC’s decision boundary is inaccurate. Yellow color sine wave just shows the underlying train data.

$$\theta^{\text{drocc}}(r) = \arg \min \|\theta\|^2, \text{ s.t.,}$$

$$\underbrace{f_\theta^{\text{drocc}}(x_i) = 1}_{\text{Positive training points}}, \underbrace{f_\theta^{\text{drocc}}(\tilde{x}_i) = -1}_{\text{Generated negatives}}, \forall \tilde{x}_i \in N_i,$$

$$N_i(r) \stackrel{\text{def}}{=} \left\{ \|\tilde{x}_i - x_i\|_2 \leq r; \|\tilde{x}_i - x_j\| \geq \gamma \cdot r, \forall j \right\}, \quad (2)$$

where N_i captures points off the manifold but are centered around x_i within a ball of radius r . Also, $\gamma \geq 0$. That is, we exclude points that are close to any training (positive) point. If the manifold is well sampled, then N_i would contain very few points from the set \mathcal{S} since such points would be close to some other point in the training set and hence excluded. Adding slack variables to allow a small amount of noise and using loss function $\ell : \mathbb{R} \times \mathbb{R} \rightarrow \mathbb{R}$, the problem can be reformulated as: $\min_\theta \ell^{\text{dr}}(\theta)$, where,

$$\ell^{\text{dr}}(\theta) = \lambda \|\theta\|^2 + \sum_{i=1}^n [\ell(f_\theta(x_i), 1) + \mu \max_{\substack{\tilde{x}_i \in \\ N_i(r)}} \ell(f_\theta(\tilde{x}_i), -1)], \quad (3)$$

and $\lambda > 0, \mu > 0$ are regularization parameters.

The formulation above is a saddle point problem and is similar to adversarial training where the network is trained to be robust to worst-case ℓ_p ball perturbations around the inputs (Madry et al., 2018). In DROCC, we replace the ℓ_p ball with $N_i(r)$, and adopt the standard projected gradient descent-ascent technique to solve the saddle point problem.

A key step in the gradient descent-ascent algorithm is that of projection onto the $N_i(r)$ set. That is, given $z \in \mathbb{R}^d$,

Algorithm 1 Training neural networks via DROCC

Input: Training data $D = [x_1, x_2, \dots, x_n]$.

Parameters: Radius r , $\lambda \geq 0$, $\mu \geq 0$, step-size η , number of gradient steps m , number of initial training steps n_0 .

Initial steps: For $B = 1, \dots, n_0$
 X_B : Batch of training inputs

$$\theta = \theta - \text{Gradient-Step} \left(\sum_{x \in X_B} \ell(f_\theta(x), 1) \right)$$

DROCC steps: For $B = n_0, \dots, n_0 + N$
 X_B : Batch of training inputs

 $\forall x \in X_B : h \sim \mathcal{N}(0, I_d)$
Adversarial search: For $i = 1, \dots, m$

$$1. \ell(h) = \ell(f_\theta(x+h), -1)$$

$$2. h = h + \eta \frac{\nabla_h \ell(h)}{\|\nabla_h \ell(h)\|}$$

$$3. h = \frac{\alpha}{\|h\|} \cdot h \text{ where } \alpha = \gamma \cdot r \cdot \mathbb{1}[\|h\| \leq \gamma \cdot r] + \|h\| \cdot \mathbb{1}[\gamma \cdot r \leq \|h\| \leq r] + r \cdot \mathbb{1}[\|h\| \geq r]$$

$$\ell^{itr} = \lambda \|\theta\|^2 + \sum_{x \in X_B} \ell(f_\theta(x), 1) + \mu \ell(f_\theta(x+h), -1)$$

$$\theta = \theta - \text{Gradient-Step}(\ell^{itr})$$

the goal is to find $\tilde{x}_i = \arg \min_x \|x - z\|^2$ s.t. $x \in N_i(r)$. Now, N_i contains points that are less than r distance away from x_i and at least $\gamma \cdot r$ away from all x_j 's. The second constraint involves all the training points and computationally challenging. So, for computational ease, we redefine $N_i(r) \stackrel{\text{def}}{=} \left\{ \gamma \cdot r \leq \|x_i - x\|_2 \leq r \right\}$. In practice, since the true normal positives \mathcal{S} lie on a low dimensional manifold, we find that the adversarial search over this set does not yield a point that is in \mathcal{S} . Further, we use a lower weight on the classification loss of the generated negatives so as to guard against possible non-anomalous points in $N_i(r)$. Finally, projection onto this set is given by $\tilde{x}_i = x_i + \alpha \cdot (z - x_i)$ where $\beta = \|z - x_i\|$, and $\alpha = r/\beta$ if $\beta \geq r$, $\alpha = \gamma \cdot r/\beta$ if $\beta \leq \gamma r$ and $\alpha = 1$ otherwise. Algorithm 1 summarizes our DROCC method. The 3 steps in the adversarial search are performed in parallel for each $x \in B$; for simplicity, we present the procedure for a single example x . Also, $\tilde{x} = x + h$. In step one, we compute the loss of the network with respect to a negative label (anomalous point). In step two, we maximize this loss in order to find the most "adversarial" point. We perform normalized steepest ascent, and finally project \tilde{x} onto $N_i(r)$. In order to update the parameters of the network, we could use any gradient based update rule such as SGD or other adaptive methods like Adagrad or Adam. We typically set $\gamma = 1/2$. Parameters λ, μ, η are selected via cross-validation. Note that our method allows arbitrary DNN architecture f_θ to represent and classify data points x_i . Finally, we select ℓ to be the standard cross-entropy loss.

4. Low-FPR One-class Classification

In this section, we formally introduce the Low-FPR One Class (LFOC) problem and extend our DROCC method

to address it. Let $D = [(x_1, y_1), \dots, (x_n, y_n)]$ be a given set of points where $x_i \in \mathbb{R}^d$ and $y_i \in \{1, -1\}$. Also, let $x_i \in \mathcal{S}$ for all i , s.t., $y_i = 1$ and $d(x_i, \mathcal{S}) \geq r$ for all points with $y_i = -1$; $d(x_i, \mathcal{S})$ is the L_2 distance between x_i and manifold \mathcal{S} . Given D , the goal is to learn a classifier f_θ that minimizes:

$$\min_{\theta} \mathbb{E}_{x \sim \mathcal{D}}[\ell(f_\theta(x), +1)] + \mathbb{E}_{x \sim \mathcal{P}}[\ell(f_\theta(x), -1)],$$

where \mathcal{D} is the distribution of positive class points, i.e., $x_i \sim \mathcal{D}$ where $y_i = 1$ and \mathcal{P} is a uniform distribution over *all* points from the negative class ($y_i = -1$). $\mathbb{E}[\cdot]$ denotes the expectation of a random variable and ℓ is a loss function defined in the previous section. So the above problem requires finding θ that has small loss over positives sampled from the *train distribution* but for negatives, we require the loss to be small wrt uniform distribution, i.e., we require strong out-of-sample generalization wrt negatives.

Intuitively, LFOC problems arise in domains where data for special positive class (or a set of classes) can be collected thoroughly but the "negative" class which is catch-all class cannot be sampled thoroughly due to its sheer size. Several real-world problems can be naturally modeled by LFOC. For example, consider wakeword problems where the goal is to identify a special audio command to wake up the system. Here, the data for a special wakeword can be collected thoroughly, but negative class which is "everything else" cannot be sampled properly. Similarly, spam detection problems can also collect "non-spam" data reasonably well, but the "spam" data cannot be sampled thoroughly because spammers might keep on changing its distribution.

Due to challenging out-of-sample generalization requirements, we rely on a similar hypothesis as the previous section, which is that the set of positive points are sampled from a low-dimensional manifold \mathcal{S} , and the negatives have distance at least $r \geq 0$ from the manifold. With this assumption, a natural baseline for this problem is where we ignore all the negative points and treat the problem as the anomaly detection problem. However, such a method requires a large number of positives and the curvature of the manifold to be small –higher curvature requires more positives– so that close points can be accurately compared using Euclidean distance. However, presence of negatives can bring down the sample complexity by allowing us to learn non-Euclidean distance functions to compare points on manifold. For example, in audio wakeword, negatives can help identify background noise as it would remain same in both positive and negative points.

More concretely, we extend formulation in (3) to allow the neighborhood set be defined via a learned elliptical distance function over the manifold. That is, our DROCC – LF method estimates parameter θ^{lf} as: $\min_{\theta} \ell^{\text{lf}}(\theta)$, where,

$$\ell^{\text{lf}}(\theta) = \lambda \|\theta\|^2 + \sum_{i=1}^n [\ell(f_\theta(x_i), y_i) + \mu \max_{\substack{\tilde{x}_i \in \\ N_i(r)}} \ell(f_\theta(\tilde{x}_i), -1)], \quad (4)$$

and $\lambda > 0$, $\mu > 0$ are regularization parameters. Similar to previous section, set $N_i(r) := \{\tilde{x}_i, s.t., \gamma \cdot r \|\tilde{x}_i - x_i\|_\Sigma \leq r\}$. However, the distance function over manifold is a Mahalanobis distance rather than the standard Euclidean distance. That is, $\|\tilde{x} - x\|_\Sigma = \sum_j \sigma_j (\tilde{x}^j - x^j)^2$ where x^j (and \tilde{x}^j) is the j -th coordinate of x (\tilde{x}) and σ_j is given by: $\sigma_j := \left| \frac{\partial f_{\theta^{init}}(x)}{\partial x_j} \right|$ for some initial-estimate θ^{init} . Note that, σ_j is proportional to "influence" of x^j on initial classifier $f_{\theta^{init}}$. Hence, if $f_{\theta^{init}}$ is learned using standard binary classification method, σ_j will decrease weight of coordinates which are mostly noisy across both positives and negatives, and it would up-weight discriminating coordinates.

Similar to (3), we can use the standard projected gradient descent-ascent algorithm to optimize the above given saddle point problem. Here again, projection onto $N_i(r)$ is the key step. That is, the goal is to find: $\tilde{x}_i = \arg \min_x \|x - z\|^2$ s.t. $x \in N_i(r)$. Unlike, Section 3 and Algorithm 1, the above projection is unlikely to be available in closed form and requires more careful arguments.

Proposition 1. *Consider the problem: $\min_{\tilde{x}} \|\tilde{x} - z\|^2$, s.t., $\|\tilde{x} - x\|_\Sigma^2 \geq r^2$ and let $\delta = z - x$. If $\|\delta\|_\Sigma^2 \geq r^2$, then $\tilde{x} = z$. Otherwise, the optimal solution is of the form: $\tilde{x} = x + (I + \tau \Sigma)^{-1} \delta$, where τ is the optimal solution to the following one-dimensional problem: $\min_{\tau \geq 0} \sum_j \frac{\delta_j^2 \tau^2 \sigma_j^2}{(1 + \tau \sigma_j)^2}$, s.t., $\sum_j \frac{\delta_j^2 \tau^2 \sigma_j^3}{(1 + \tau \sigma_j)^2} \geq r^2$.*

See Appendix A for a detailed proof. The above proposition reduces the projection problem to a non-convex but one-dimensional optimization problem. We solve this problem via standard grid search over: $\tau = [0, -\frac{1}{\max_j \sigma_j}]$. The algorithm is now almost same as Algorithm 1 but uses the above mentioned projection algorithm; see Appendix A for a pseudo-code of our DROCC – LF method.

5. Empirical Evaluation

In this section, we present empirical evaluation of the DROCC approach on two one-class classification problems: Anomaly Detection (AD) and Low FPR Classification (LFOC). We discuss the experimental setup, datasets, baselines, and the implementation details. Through experimental results on a wide range of synthetic and real-world datasets, we present strong empirical evidence for the effectiveness of our approach for one-class classification.

5.1. Anomaly Detection

Datasets: In all the experiments with multi-class datasets, we follow the standard procedure to convert them into anomaly detection problems: fixing each class as nominal and treat rest as anomaly. The model is trained only on the nominal class but the test data is sampled from all the classes. For timeseries datasets, N represents the number of

time-steps/frames and d represents the input feature length.

We perform experiments on the following datasets:

- 2-D sine-wave: this data contains 1000 points sampled uniformly from a 2-dimensional sine wave (see Figure 1a).
- CIFAR-10 (Krizhevsky, 2009): a widely used benchmark for anomaly detection. CIFAR-10 has 10 different classes with 32×32 color images.
- ImageNet-10: a subset of 10 randomly chosen classes from the ImageNet dataset (Deng et al., 2009) which contains 224×224 color images.
- Epileptic Seizure Recognition (Andrzejak et al., 2001): EEG based time-series from multiple patients. The task is to identify if EEG is abnormal ($N = 178$, $d = 1$).
- HAR-2 (Anguita et al., 2012): accelerometer and gyroscope readings from a smartphone for the task of human activity recognition ($N = 128$, $d = 9$).
- Audio Commands (Warden, 2018): a multiclass data with 35 classes of audio keywords. Data is featurized using standard MFCC features with 32 filter banks over 25ms length windows with stride of 10ms ($N = 98$, $d = 32$).

The datasets which we use are all publicly available. We use the train-test splits when already available with a 80-20 split for train and validation set. In all other cases, we use random 60-20-20 split for train, validation and test.

Metric: To evaluate our method and benchmark it against prior work, we use the standard area under the ROC curve (AUC) as the metric for all the AD experiments, which is given by the fraction of pairs of normal and abnormal points where the learned scoring function ranks normal points above the abnormal points.

Baselines and Implementation: We use the standard nearest neighbours, autoencoder, and DeepSVDD as baselines. The number of nearest neighbors k is tuned over the validation set. Motivated by recent analysis (Gu et al., 2019), we include nearest neighbours as one of the baselines, despite its omission in prior works. The anomaly score for each test point is defined as the mean distance of the test point from the nearest k -training points. The value of k is tuned for each dataset and the highest AUC values are reported. In addition to nearest neighbours, we use autoencoders and DeepSVDD as baselines. The architecture for the encoder of the autoencoder, the network in DeepSVDD and the network for DROCC is kept same to maintain consistency in results. The decoder of the autoencoder is constructed by reversing the architecture of the encoder. The encoding dimension for the autoencoder and DeepSVDD (dimension of the representation to which one-class loss is applied) is tuned for each dataset. For each of the method, we also tune the weight decay parameter $5 \cdot \{10^{-4}, 10^{-5}, 10^{-7}\}$.

DROCC: The main hyper-parameter of our algorithm is

Table 1. Average AUC (with standard deviation) for one-vs-all anomaly detection on CIFAR-10. DROCC outperforms baselines on most classes, with gains as high as 20%, and notably, nearest neighbours beats all the baselines on 2 classes.

CIFAR Class	OC-SVM	IF	DCAE	AnoGAN	ConAD 16	Soft-Bound Deep SVDD	One-Class Deep SVDD	Nearest Neighbour	DROCC (Ours)
Airplane	61.6±0.9	60.1±0.7	59.1±5.1	67.1±2.5	77.2	61.7±4.2	61.7±4.1	69.02	81.66 ± 0.22
Automobile	63.8±0.6	50.8±0.6	57.4±2.9	54.7±3.4	63.1	64.8±1.4	65.9±2.1	44.2	76.738 ± 0.99
Bird	50.0±0.5	49.2±0.4	48.9±2.4	52.9±3.0	63.1	49.5±1.4	50.8±0.8	68.27	66.664 ± 0.96
Cat	55.9±1.3	55.1±0.4	58.4±1.2	54.5±1.9	61.5	56.0±1.1	59.1±1.4	51.32	67.132 ± 1.51
Deer	66.0±0.7	49.8±0.4	54.0±1.3	65.1±3.2	63.3	59.1±1.1	60.9±1.1	76.71	73.624 ± 2.00
Dog	62.4±0.8	58.5±0.4	62.2±1.8	60.3±2.6	58.8	62.1±2.4	65.7±2.5	49.97	74.434 ± 1.95
Frog	74.7±0.3	42.9±0.6	51.2±5.2	58.5±1.4	69.1	67.8±2.4	67.7±2.6	72.44	74.426 ± 0.92
Horse	62.6±0.6	55.1±0.7	58.6±2.9	62.5±0.8	64.0	65.2±1.0	67.3±0.9	51.13	71.39 ± 0.22
Ship	74.9±0.4	74.2±0.6	76.8±1.4	75.8±4.1	75.5	75.611.7	75.9±1.2	69.09	80.016 ± 1.69
Truck	75.9±0.3	58.9±0.7	67.3±3.0	66.5±2.8	63.7	71.0±1.1	73.1±1.2	43.33	76.21 ± 0.67

the radius $\gamma \cdot r$ of the ball outside which we sample negative points. We observe that tweaking radius value around $\sqrt{d}/2$ (where d is the dimension of the input data) works the best, as due to zero-mean, unit-variance normalized features, the average distance between random points is $\approx \sqrt{d}$. Parameter μ (3) is chosen from $\{0.1, 0.25, 0.75, 1.0\}$. We use a standard step size from $\{0.1, 0.01\}$ for gradient ascent and from $\{10^{-2}, 10^{-4}\}$ for gradient descent; we also tune the optimizer $\in \{\text{Adam, SGD}\}$. The experiments were run on an Intel Xeon CPU with 12 cores clocked at 2.60 GHz and with NVIDIA Tesla P40 GPU, CUDA 10.0 and cuDNN 7.6. See Appendix D for a detailed ablation study.

5.1.1. RESULTS

Synthetic Data: We first present results on a simple 2-D sine wave dataset to visualize the kind of classifiers learnt by DROCC. Here, the positive data points lie on the 1-D manifold given in Figure 1a. We observe from Figure 1b that DROCC is able to capture the manifold structure accurately; whereas the classical methods OC-SVM and DeepSVDD (shown in Appendix B) perform poorly as they both try to learn a minimum enclosing ball for the *whole* set of positive data points.

Image Data: Table 1 presents comparisons on CIFAR10 for DROCC against baseline numbers OC-SVM, IF, DCAE, AnoGAN, and DeepSVDD as reported by Ruff et al. (2018) and against ConvAD16 as reported by Nguyen et al. (2019). LeNet (LeCun et al., 1998) architecture was used for all the baselines and DROCC for this experiment. DROCC consistently achieves the best performance on most of the classes, with gains as high as 20% over DeepSVDD on some classes. An interesting observation is that for the classes Bird and Deer, Nearest Neighbour achieves competitive performance, beating all the other baselines.

Next, we benchmark the performance of DROCC on high resolution images which require use of large modern neural architectures. Table 2 presents the results of our experiments on ImageNet. DROCC continues to achieve the best results amongst all the compared methods. Autoencoder fails drastically on this dataset, so we exclude comparisons. For DeepSVDD and DROCC, MobileNetv2 (Sandler et al.,

2018b) architecture is used. We observe that for all classes, except golf ball, DROCC outperforms the baselines. For instance, on French-Horn vs rest problem, DROCC is 23% more accurate than DeepSVDD.

Time-Series Data: Prior work on deep anomaly detection in general lacks evaluation on time-series data which arise naturally in many real-world settings. We perform extensive experiments on a broad range of time-series data. A single layer LSTM network is used for all the experiments with time series. For autoencoders, we use the architecture presented in Srivastava et al. (2015). Figure 2a compares the performance of DROCC against Nearest Neighbours, Autoencoders and DeepSVDD baselines on the univariate Epileptic Seizure dataset. There are two key observations from the results. First, DROCC outperforms the baselines for all values of the LSTM hidden dimension. That is, DROCC is able to achieve 98% AUC, while DeepSVDD and Autoencoders obtain accuracy of 94% and 92%, respectively. Second, DROCC shows increase in performance with hidden dimension, whereas the performances of DeepSVDD and Autoencoder degrades after a threshold. Similar observations hold true for the HAR-2 dataset (Figure 2b) as well as the Audio Commands dataset (Figure 2c), where we cast the problem as “Marvin” vs rest-keywords.

5.2. Low-FPR Classification (LFOC)

Recall that the goal in LFOC is to learn a classifier that is accurate for both, the in-sample positive (or normal) class points and for the arbitrary out-of-distribution (OOD) negatives. Naturally, the key metric for this problem is False

Table 2. Average AUC (with standard deviation) for one-vs-all anomaly detection on ImageNet. DROCC consistently achieves the best performance for all but one class.

ImageNet Class	Nearest Neighbor	DeepSVDD	DROCC (Ours)
Tench	65.57	65.14 ± 1.03	70.19 ± 1.7
English Springer	56.37	66.45 ± 3.16	70.45 ± 4.99
Cassette Player	47.7	60.47 ± 5.35	71.17 ± 1
Chainsaw	45.22	59.43 ± 4.13	68.63 ± 1.86
Church	61.35	56.31 ± 4.23	67.46 ± 4.17
French Horn	50.52	53.06 ± 6.52	76.97 ± 1.67
Garbage Truck	54.2	62.15 ± 4.39	69.06 ± 2.34
Gas Pump	47.43	56.66 ± 1.49	69.94 ± 0.57
Golf Ball	70.36	72.23 ± 3.43	70.72 ± 3.83
Parachute	75.87	81.35 ± 3.73	93.5 ± 1.41

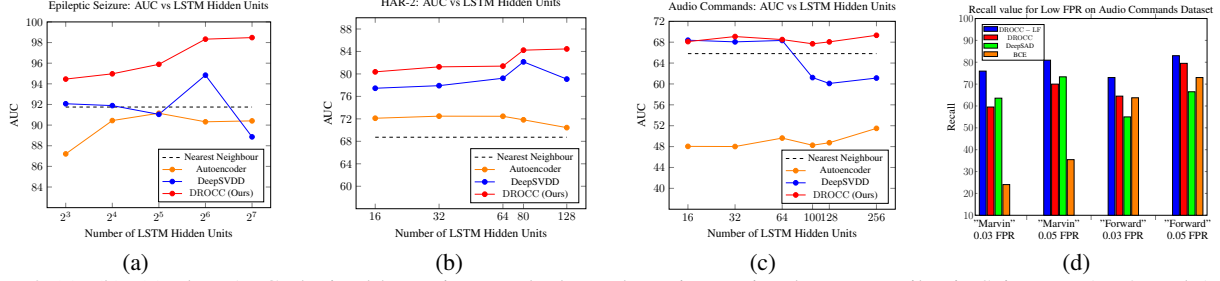


Figure 2. (a), (b), (c) plots AUC obtained by various methods on three time-series datasets: Epileptic Seizure, HAR-2, and Audio Commands. DROCC consistently outperforms the baselines, e.g., for HAR-2, DROCC is 6% more accurate than baselines. Furthermore, as expected, DeepSVDD and Autoencoder become unstable for larger number of LSTM hidden units. (d) LFOC on Audio Commands: comparison of recall obtained by different methods for two keywords “Marvin” and “Forward” when the False Positive Rate (FPR) is fixed to be 3% and 5%. DROCC – LF is consistently about 10% more accurate than all the baselines.

Positive Rate (FPR). In our experiments, we bound any method to have FPR to be smaller than a threshold and under that constraint, we measure it’s recall value, i.e., the fraction of true positives that are correctly predicted.

We compare DROCC – LF against the following baselines: a) Standard binary classifier: that is, we ignore the challenge of OOD negatives and treat the problem as a standard classification task, b) DROCC: here we ignore the provided negatives and focus only on modeling positives, c) DeepSAD (Ruff et al., 2020): a semi-supervised anomaly detection method but it is not explicitly designed to handle negatives that are very close to positives (OOD negatives). Similar to the anomaly detection experiments, we use the same underlying network architecture across all the baselines.

5.2.1. RESULTS

Synthetic Data: We sample 1024 points in \mathbb{R}^{10} where the first two coordinates are sampled from the 2D-sine wave, as in the previous section. Coordinates 3 to 10 are sampled from the spherical Gaussian distribution. Note that due to the 8 noisy dimensions, DROCC would be forced to set $\gamma \cdot r = \sqrt{d}$ where $d = 10$, while the true low-dimensional manifold is restricted to only two dimensions. Consequently, it learns an inaccurate boundary as shown in Figure 1c and is similar to the boundary learned by OC-SVM and DeepSVDD; points that are predicted to be positive by DROCC are colored blue. In contrast, DROCC – LF is able to learn that only the first two coordinates are useful for distinction between positives and negatives, and hence is able to learn a skewed distance function, leading to an accurate decision boundary (see Figure 1d).

Wakeword Detection: Finally, we evaluate DROCC – LF on the practical problem of wakeword detection with low FPR against arbitrary OOD negatives. To this end, we identified a keyword “Marvin” from the audio commands dataset (Warden, 2018) as the *positive* class and the remaining 34 keywords are labeled as the negative class. For training, we

sample points uniformly at random from the above mentioned dataset. However, for evaluating the solution, we sample positives from the train distribution but negatives contain a few challenging OOD points as well. Sampling challenging negatives itself is a hard task and is the key motivating reason for studying the problem. So, we manually list close-by keywords to *Marvin* such as: *Mar*, *Vin*, *Marvelous* etc. We then generate audio snippets for these keywords via a speech synthesis tool with a variety of accents.

Finally, we compare the recall of DROCC – LF against that of baselines for fixed FPR: a) 3%, b) 5%. Figure 2d shows that for both the FPR settings, DROCC – LF is significantly more accurate than the baselines. For example, with FPR=3%, DROCC – LF is 10% more accurate than the baselines. We repeated the same experiment with one more keyword: *Forward*, and observed similar trend. In summary, DROCC – LF is able to generalize well against negatives that are “close” to the true positives even when such negatives were not supplied with the training data.

6. Conclusions

We introduced DROCC method for deep anomaly detection. It models normal data points using a low-dimensional manifold, and hence can compare close point via Euclidean distance. Based on this intuition, DROCC’s optimization is formulated as a saddle point problem which is solved via standard gradient descent-ascent algorithm. We then extended DROCC to LFOC problem where the goal is to generalize well against *arbitrary* negatives, assuming positive class is well sampled and a small number of negative points are also available. Both the methods perform significantly better than strong baselines, in their respective problem settings. For computational efficiency, we simplified the projection set for both the methods which can perhaps slow down the convergence of the two methods. Designing optimization algorithms that can work with the stricter set is an exciting research direction. Further, we would also like to rigorously analyse DROCC, assuming

enough samples from a low-curvature manifold. Finally, as LFOC is an exciting problem that routinely comes up in a variety of real-world applications, we would like to apply DROCC – LF to a few high impact scenarios.

7. Acknowledgments

We are grateful to Aditya Kusupati, Nagarajan Natarajan, Sahil Bhatia and Oindrila Saha for helpful discussions and feedback.

References

- Andrzejak, R. G., Lehnertz, K., Mormann, F., Rieke, C., David, P., and Elger, C. E. Indications of nonlinear deterministic and finite-dimensional structures in time series of brain electrical activity: Dependence on recording region and brain state. *Physical Review E*, 64(6), 2001.
- Anguita, D., Ghio, A., Oneto, L., Parra, X., and Reyes-Ortiz, J. L. Human activity recognition on smartphones using a multiclass hardware-friendly support vector machine. In *International Workshop on Ambient Assisted Living*, 2012.
- Bergman, L. and Hoshen, Y. Classification-based anomaly detection for general data. In *International Conference on Learning Representations (ICLR)*, 2020.
- Boyd, S. and Vandenberghe, L. *Convex Optimization*. Cambridge University Press, USA, 2004. ISBN 0521833787.
- Chandola, V., Banerjee, A., and Kumar, V. Anomaly detection: A survey. *ACM Computing Surveys (CSUR)*, 41(3), 2009.
- Deng, J., Dong, W., Socher, R., Li, L.-J., Li, K., and Fei-Fei, L. Imagenet: A large-scale hierarchical image database. In *IEEE Conference on Computer Vision and Pattern Recognition (CVPR)*, 2009.
- Golan, I. and El-Yaniv, R. Deep anomaly detection using geometric transformations. In *Advances in Neural Information Processing Systems (NeurIPS)*, 2018.
- Goldstein, M. and Uchida, S. A comparative evaluation of unsupervised anomaly detection algorithms for multivariate data. *PLOS ONE*, 11(4), 2016.
- Gu, X., Akoglu, L., and Rinaldo, A. Statistical analysis of nearest neighbor methods for anomaly detection. In *Advances in Neural Information Processing Systems (NeurIPS)*, 2019.
- Hendrycks, D. and Gimpel, K. A baseline for detecting misclassified and out-of-distribution examples in neural networks. *CoRR*, abs/1610.02136, 2016. URL <http://arxiv.org/abs/1610.02136>.
- Hendrycks, D., Mazeika, M., and Dietterich, T. Deep anomaly detection with outlier exposure. In *International Conference on Learning Representations (ICLR)*, 2019a.
- Hendrycks, D., Mazeika, M., Kadavath, S., and Song, D. Using self-supervised learning can improve model robustness and uncertainty. In *Advances in Neural Information Processing Systems (NeurIPS)*, 2019b.
- Krizhevsky, A. Learning multiple layers of features from tiny images, 2009.
- Lakhina, A., Crovella, M., and Diot, C. Diagnosing network-wide traffic anomalies. *SIGCOMM Comput. Commun. Rev.*, 34(4), 2004.
- LeCun, Y., Bottou, L., Bengio, Y., and Haffner, P. Gradient-based learning applied to document recognition. *Proceedings of the IEEE*, 86(11), 1998.
- Liu, F. T., Ting, K. M., and Zhou, Z.-H. Isolation forest. In *Proceedings of the 2008 Eighth IEEE International Conference on Data Mining*, 2008.
- Madry, A., Makelov, A., Schmidt, L., Tsipras, D., and Vladu, A. Towards deep learning models resistant to adversarial attacks. In *International Conference on Learning Representations (ICLR)*, 2018.
- Malhotra, P., Ramakrishnan, A., Anand, G., Vig, L., Agarwal, P., and Shroff, G. Lstm-based encoder-decoder for multi-sensor anomaly detection, 2016. URL <https://arxiv.org/abs/1607.00148>.
- Nguyen, D. T., Lou, Z., Klar, M., and Brox, T. Anomaly detection with multiple-hypotheses predictions. In *International Conference on Machine Learning (ICML)*, 2019.
- Pless, R. and Souvenir, R. A survey of manifold learning for images. *IPSJ Transactions on Computer Vision and Applications*, 1, 2009.
- Ruff, L., Vandermeulen, R., Goernitz, N., Deecke, L., Siddiqui, S. A., Binder, A., Müller, E., and Kloft, M. Deep one-class classification. In *International Conference on Machine Learning (ICML)*, 2018.
- Ruff, L., Vandermeulen, R. A., Goernitz, N., Binder, A., Müller, E., Müller, K.-R., and Kloft, M. Deep semi-supervised anomaly detection. In *International Conference on Learning Representations (ICLR)*, 2020.
- Sakurada, M. and Yairi, T. Anomaly detection using autoencoders with nonlinear dimensionality reduction. In *Proceedings of the MLSDA 2014 2nd Workshop on Machine Learning for Sensory Data Analysis*, 2014.

- Sandler, M., Howard, A., Zhu, M., Zhmoginov, A., and Chen, L.-C. Mobilenetv2: Inverted residuals and linear bottlenecks, 2018a. URL <https://arxiv.org/abs/1801.04381>.
- Sandler, M., Howard, A., Zhu, M., Zhmoginov, A., and Chen, L.-C. Mobilenetv2: Inverted residuals and linear bottlenecks. In *IEEE Conference on Computer Vision and Pattern Recognition (CVPR)*, 2018b.
- Schölkopf, B., Williamson, R., Smola, A., Shawe-Taylor, J., and Platt, J. Support vector method for novelty detection. In *Proceedings of the 12th International Conference on Neural Information Processing Systems*, 1999.
- Srivastava, N., Mansimov, E., and Salakhudinov, R. Unsupervised learning of video representations using lstms. In *International Conference on Machine Learning (ICML)*, 2015.
- Tax, D. M. and Duin, R. P. Support vector data description. *Machine Learning*, 54(1), 2004.
- Warden, P. Speech commands: A dataset for limited-vocabulary speech recognition, 2018. URL <https://arxiv.org/abs/1804.03209>.

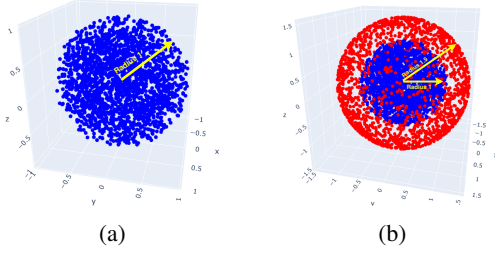


Figure 3. (a) Spherical manifold (a unit sphere) that captures the normal data distribution. Points are uniformly sampled from the volume of the unit sphere. (b) OOD points (red) are sampled on the *surface* of a sphere of varying radius. Table 3 shows AUC values with varying radius.

A. LFOC Proof

Proof of Proposition 1. Recall the problem:

$$\min_{\tilde{x}} \|\tilde{x} - z\|^2, \text{ s.t. }, \|\tilde{x} - x\|_{\Sigma}^2 \geq r^2.$$

Let $\tau \leq 0$ be the Lagrangian multiplier, then the Lagrangian function of the above problem is given by:

$$L(\tilde{x}, \tau) = \|\tilde{x} - z\|^2 + \tau(\|\tilde{x} - x\|_{\Sigma}^2 - r^2).$$

Using KKT first-order necessary condition (Boyd & Vandenberghe, 2004), the following should hold for any optimal solution \tilde{x}, τ :

$$\nabla_{\tilde{x}} L(\tilde{x}, \tau) = 0.$$

That is,

$$\tilde{x} = (I + \tau\Sigma)^{-1}(z + \tau \cdot \Sigma x) = x + (I + \tau \cdot \Sigma)^{-1}\delta,$$

where $\delta = z - x$. This proves the first part of the lemma.

Now, by using primal and dual feasibility required by the KKT conditions, we have:

$$\min_{\tau \leq 0} \|\tilde{x} - z\|^2, \text{ s.t. }, \|\tilde{x} - x\|_{\Sigma}^2 \geq r^2,$$

where $\tilde{x} = (I + \tau\Sigma)^{-1}(z + \tau \cdot \Sigma x) = x + (I + \tau \cdot \Sigma)^{-1}\delta$. The lemma now follows by substituting \tilde{x} above and by using the fact that Σ is a diagonal matrix with $\Sigma(i, i) = \sigma_i$. \square

B. Synthetic Experiments

B.1. 1-D Sine Manifold

In Section 5.1.1 we presented results on a synthetic dataset of 1024 points sampled from a 1-D sine wave (See Figure 1a). We compare DROCC to other anomaly detection methods by plotting the decision boundaries on this same dataset. Figure 4 shows the decision boundary for a) DROCC b) OC-SVM with RBF kernel c) OC-SVM with 20-degree polynomial kernel d) DeepSVDD. All methods are trained only on positive points from the 1-D manifold.

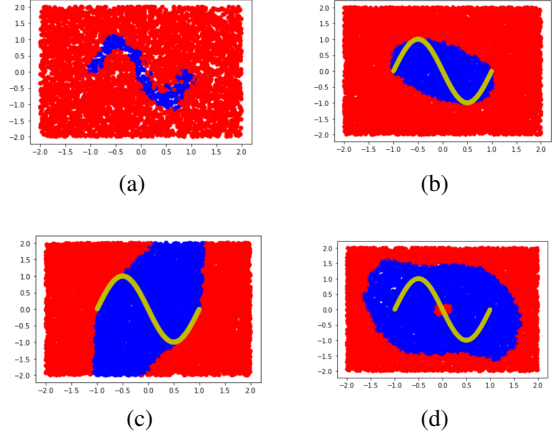


Figure 4. (a) Decision boundary of DROCC trained only on the positive points lying on the 1-D sine manifold in Figure 1a. Blue represents points classified as normal and red classified as abnormal. (b) Decision boundary of classical OC-SVM using RBF kernel and same experiment settings as in (a). Yellow sine wave just shows the underlying train data. (c) Decision boundary of classical OC-SVM using a 20-degree polynomial kernel. (d) Decision boundary of DeepSVDD.

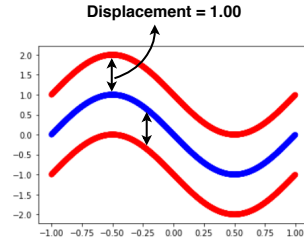


Figure 5. Illustration of the negative points sampled at various displacements of the sine wave; used for reporting the AUC values in the Table 4. In this figure, vertical displacement is 1.0. Blue represents the positive points (also the training data) and red represents the negative/OOD points

We further evaluate these methods for varied sampling of negative points near the positive manifold. Negative points are sampled from a 1-D sine manifold vertically displaced in both the directions (See Figure 5). Table 4 compares DROCC against various baselines on this dataset.

B.2. Spherical Manifold

OC-SVM and DeepSVDD try to find a minimum enclosing ball for the whole set of positive points, while DROCC assumes that the true points low on a low dimensional manifold. We now test these methods on a different synthetic dataset: spherical manifold where the positive points are within a sphere, as shown in Figure 3a. Normal/Positive points are sampled uniformly from the volume of the unit sphere. Table 3 compares DROCC against various baselines when the OOD points are sampled on the *surface* of

Table 3. Average AUC for Spherical manifold experiment (Section B.2). Normal points are sampled uniformly from the volume of a unit sphere and OOD points are sampled from the *surface* of a unit sphere of varying radius (See Figure 3b). Again DROCC outperforms all the baselines when the OOD points are quite close to the normal distribution.

Radius	Nearest Neighbor	OC-SVM	AutoEncoder	DeepSVDD	DROCC (Ours)
1.2	100 \pm 0.00	92.00 \pm 0.00	91.81 \pm 2.12	93.26 \pm 0.91	99.44 \pm 0.10
1.4	100 \pm 0.00	92.97 \pm 0.00	97.85 \pm 1.41	98.81 \pm 0.34	99.99 \pm 0.00
1.6	100 \pm 0.00	92.97 \pm 0.00	99.92 \pm 0.11	99.99 \pm 0.00	100.00 \pm 0.00
1.8	100 \pm 0.00	91.87 \pm 0.00	99.98 \pm 0.04	100.00 \pm 0.00	100.00 \pm 0.00
2.0	100 \pm 0.00	91.83 \pm 0.00	100 \pm 0.00	100.00 \pm 0.00	100.00 \pm 0.00

Table 4. Average AUC for the synthetic 1-D Sine Wave manifold experiment (Section B.1). Normal points are sampled from a sine wave and OOD points from a vertically displaced manifold (See Figure 5). The results demonstrate that only DROCC is able to capture the manifold tightly

Vertical Displacement	Nearest Neighbor	OC-SVM	AutoEncoder	DeepSVDD	DROCC (Ours)
0.2	100 \pm 0.00	56.99 \pm 0.00	52.48 \pm 1.15	65.91 \pm 0.64	96.80 \pm 0.65
0.4	100 \pm 0.00	68.84 \pm 0.00	58.59 \pm 0.61	78.18 \pm 1.67	99.31 \pm 0.80
0.6	100 \pm 0.00	76.95 \pm 0.00	66.59 \pm 1.21	82.85 \pm 1.96	99.92 \pm 0.11
0.8	100 \pm 0.00	81.73 \pm 0.00	77.42 \pm 3.62	86.26 \pm 1.69	99.98 \pm 0.01
1.0	100 \pm 0.00	88.18 \pm 0.00	86.14 \pm 2.52	90.51 \pm 2.62	100 \pm 0.00
2.0	100 \pm 0.00	98.56 \pm 0.00	100 \pm 0.00	100 \pm 0.00	100 \pm 0.00

Table 5. Ablation Study on CIFAR-10: Sampling negative points randomly in the set $N_i(r)$ (DROCC – Random) instead of gradient ascent (DROCC).

CIFAR Class	One-Class Deep SVDD	DROCC	DROCC – Random
Airplane	61.7 \pm 4.1	81.66 \pm 0.22	79.67 \pm 2.09
Automobile	65.9 \pm 2.1	76.74 \pm 0.99	73.48 \pm 1.44
Bird	50.8 \pm 0.8	66.66 \pm 0.96	62.76 \pm 1.59
Cat	59.1 \pm 1.4	67.13 \pm 1.51	67.33 \pm 0.72
Deer	60.9 \pm 1.1	73.62 \pm 2.00	56.09 \pm 1.19
Dog	65.7 \pm 2.5	74.43 \pm 1.95	65.88 \pm 0.64
Frog	67.7 \pm 2.6	74.43 \pm 0.92	74.82 \pm 1.77
Horse	67.3 \pm 0.9	71.39 \pm 0.22	62.08 \pm 2.03
Ship	75.9 \pm 1.2	80.01 \pm 1.69	80.04 \pm 1.71
Truck	73.1 \pm 1.2	76.21 \pm 0.67	70.80 \pm 2.73

Table 6. Ablation Study on HAR-2 time-series dataset: Sampling negative points randomly in the set $N_i(r)$ (DROCC – Random) instead of gradient ascent (DROCC).

LSTM Hidden Dimension	One-Class Deep SVDD	DROCC	DROCC – Random
128	79.08	84.45	81.21
80	82.15	84.23	81.08
64	79.23	81.39	81.72
32	77.91	81.26	78.82
16	77.45	80.37	81.67

a sphere of varying radius (See Figure 3b). DROCC again outperforms all the baselines even in the case when minimum enclosing ball would suit the best. Suppose instead of neural networks, we were operating with purely linear models, then DROCC also essentially finds the minimum enclosing ball (for a suitable radius r). If r is too small, the training doesn’t converge since there is no separating boundary). Assuming neural networks are implicitly regularized to find the simplest boundary, DROCC with neural networks also learns essentially a minimum enclosing ball in this case, however at a slightly larger radius. Therefore, we get 100% AUC only at radius 1.6 rather than $1 + \epsilon$ for some very small ϵ .

Table 7. Synthesized near-negatives for keywords in Audio Commands

Marvin	Forward	Seven	Follow
mar	for	one	fall
marlin	fervor	eleven	fellow
arvin	ward	heaven	low
marvik	reward	when	hollow
arvi	onward	devon	wallow

Table 8. Hyperparameters: CIFAR-10

Class	Radius	μ	Optimizer	Learning Rate	Adversarial Ascent Step Size
Airplane	8	1	Adam	0.001	0.001
Automobile	32	0.5	SGD (M)	0.01	0.001
Bird	40	0.5	Adam	0.001	0.001
Cat	16	0.5	SGD (M)	0.001	0.001
Deer	16	1	SGD (M)	0.001	0.001
Dog	24	0.5	SGD (M)	0.01	0.001
Frog	24	0.5	Adam	0.01	0.001
Horse	24	0.5	SGD (M)	0.01	0.001
Ship	48	1	Adam	0.01	0.001
Truck	16	1	SGD (M)	0.001	0.001

C. LFOC Supplementary Experiments

In Section 5.2.1, we compared DROCC – LF with various baselines for the LFOC task where the goal is to learn a classifier that is accurate for both the positive class and the arbitrary OOD negatives. Figure 8 compares the recall obtained by different methods on 2 keywords ”Seven” and ”Follow” with 2 different FPR. Table 7 lists the close negatives which were synthesized for each of the keyword.

D. Ablation Study

D.1. Hyper-Parameters

Here we analyze the effect of two important hyperparameters — radius r of the ball outside which we sample negative points and μ which is the weightage given to the

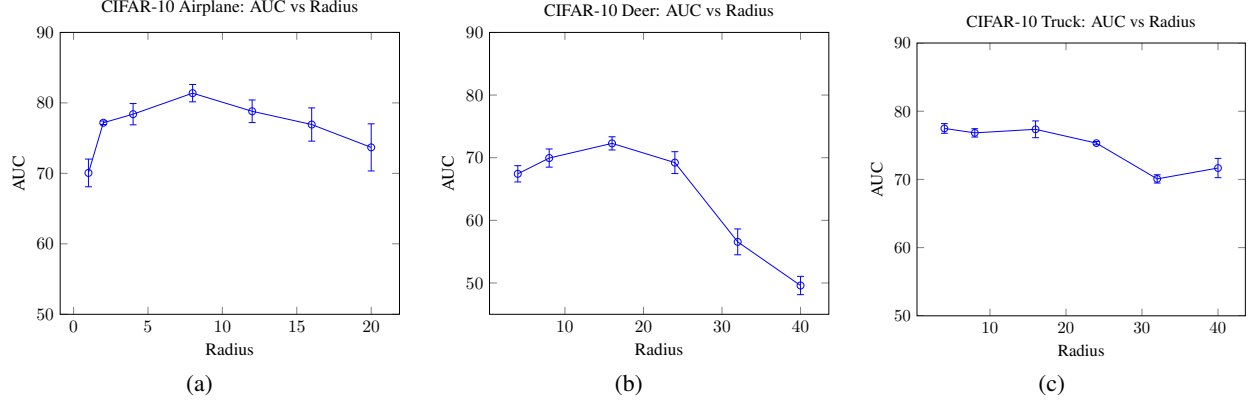


Figure 6. Ablation Study : Variation in the performance DROCC when $\gamma \cdot r$ (with $\gamma = 1/2$) is changed from the optimal value.

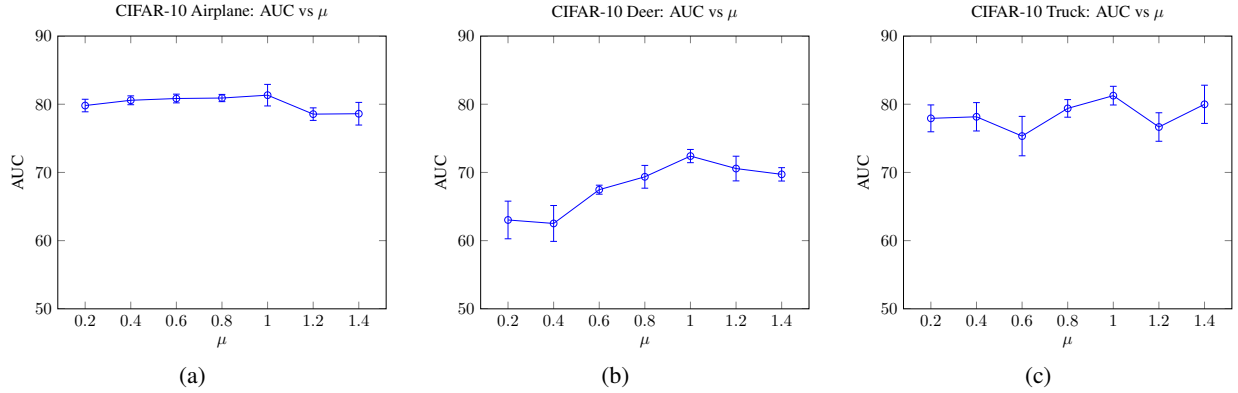


Figure 7. Ablation Study : Variation in the performance of DROCC with μ (3) which is the weightage given to the loss from adversarially sampled negative points

Table 9. Hyperparameters: ImageNet

Class	Radius	μ	Optimizer	Learning Rate	Adversarial Ascent Step Size
Tench	30	1	SGD (M)	0.01	0.001
English_springer	16	1	SGD (M)	0.001	0.001
Cassette_player	40	1	Adam	0.005	0.001
Chain_saw	20	1	SGD (M)	0.01	0.001
Church	40	1	Adam	0.01	0.001
French_horn	20	1	SGD (M)	0.05	0.001
Garbage_truck	30	1	Adam	0.005	0.001
Gas_pump	30	1	Adam	0.01	0.001
Golf_ball	30	1	SGD (M)	0.01	0.001
Parachute	12	1	Adam	0.001	0.001

loss from adversarially sampled negative points (See Equation 3). We set $\gamma = 1/2$ and recall that the negative points are sampled to be at distance between $\gamma \cdot r$ and r of positive points.

Figure 6a, 6b and 6c show the performance of DROCC with varied values of r on the CIFAR-10 dataset. The graphs demonstrate that sampling negative points quite far from the manifold (setting r to be very large), causes a drop in the accuracy since now DROCC would be covering the normal data manifold loosely causing high false positives. At the

Table 10. Hyperparameters: Epilepsy

LSTM Hidden Units	Radius	μ	Optimizer	Learning Rate	Adversarial Ascent Step Size
8	2	0.5	Adam	10^{-4}	0.1
16	6	0.5	Adam	10^{-4}	0.1
32	16	0.5	Adam	10^{-4}	0.1
64	12	1	Adam	10^{-5}	0.1
128	13	0.5	Adam	10^{-5}	0.1

Table 11. Hyperparameters: HAR-2

LSTM Hidden Units	Radius	μ	Optimizer	Learning Rate	Adversarial Ascent Step Size
16	40	1	Adam	0.01	0.01
32	30	0.5	Adam	0.001	0.01
64	25	1	Adam	0.01	0.01
80	25	1	Adam	0.01	0.01
128	40	0.75	Adam	0.01	0.01

other extreme, if the radius is set too small, the decision boundary could be too close to the positive and hence lead to overfitting and difficulty in training the neural network.

Figure 7a, 7b and 7c show the effect of μ on the performance of DROCC on CIFAR-10.

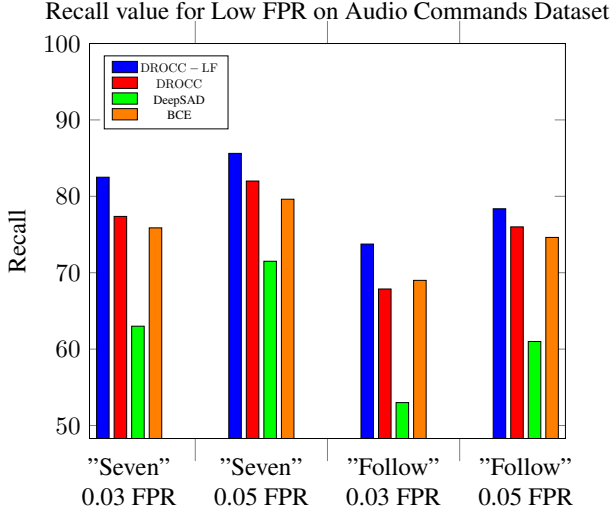


Figure 8. LFOC on Audio Commands: Recall obtained by different methods for two keywords “Seven” and “Follow” when the False Positive Rate (FPR) is fixed to be 3% and 5%. DROCC – LF is consistently about 7% more accurate than all the baselines.

Table 12. Hyperparameters: Anomaly Detection with Keyword *Marvin*

LSTM Hidden Units	Radius	μ	Optimizer	Learning Rate	Adversarial Ascent Step Size
16	80	1	Adam	0.0001	0.1
32	60	1	Adam	0.0001	0.1
64	40	0.75	Adam	0.0001	0.1
100	10	0.75	Adam	0.001	0.1
128	80	1	Adam	0.001	0.1
256	60	1	Adam	0.0001	0.1

D.2. Importance of gradient ascent-descent technique

In the Section 3.2 we formulated the DROCC’s optimization objective as a saddle point problem (Equation 3). We adopted the standard gradient descent-ascent technique to solve the problem replacing the ℓ_p ball with $N_i(r)$. Here, we present an analysis of DROCC without the gradient ascent part i.e. we now sample points at random in the set of negatives $N_i(r)$. We call this formulation as DROCC – Random. Table 5 shows the drop in performance when negative points are sampled randomly on the CIFAR-10, hence emphasizing the importance of gradient ascent-descent technique. Since $N_i(r)$ is high dimensional, random sampling does not find points close enough to manifold of positive points. Table 6 presents the same analysis on the HAR time-series dataset.

Table 13. Hyperparameters: LFOC Experiments

Keyword	Radius	μ	Optimizer	Learning Rate	Adversarial Ascent Step Size
Marvin	0.5	0.1	Adam	0.001	0.01
Forward	0.8	0.05	Adam	0.001	0.01
Seven	0.5	0.1	Adam	0.005	0.01
Follow	1.5	0.05	Adam	0.005	0.01

E. Experiment details and Hyper-Parameters for Reproducibility

E.1. CIFAR-10

DeepSVDD uses the representations learnt in the penultimate layer of LeNet (LeCun et al., 1998) for minimizing their one-class objective. To make a fair comparison we use the same base architecture. However, since DROCC formulates the problem as a binary classification task, we add a final fully connected layer over the learned representations to get the binary classification scores. Table 8 lists the hyper-parameters which were used to run the experiments on the standard test split of CIFAR-10.

E.2. ImageNet-10

MobileNet2 (Sandler et al., 2018a) was used as the base architecture for DeepSVDD and DROCC. Again we use the representations from the penultimate layer of MobileNet2 for optimizing the one-class objective of DeepSVDD. The width multiplier for MobileNet2 was set to be 1.0. Table 9 lists all the hyper-parameters.

E.3. Time Series Datasets

To keep the focus only on comparing DROCC against the baseline formulations for OOD detection, we use a single layer LSTM for all the experiments on Epileptic Seizure Detection dataset, HAR dataset and the Audio Commands dataset. The hidden state from the last time step is used for optimizing the one class objective of DeepSVDD. For DROCC we add a fully connected layer over the last hidden state to get the binary classification scores. Table 10, 11 and 12 list all the hyper-parameters for reproducibility.

E.4. LFOC Experiments on Audio Commands

For the Low-FPR classification task we use keywords from the Audio Commands dataset along with some synthesized near-negatives. The training set consists of 1000 examples each of the keyword and equal randomly samples examples from the remaining classes in the dataset. The validation and test set consist of 200 examples of the keyword, same number of words from other classes of Audio Commands dataset and a extra synthesized 200 examples of close negatives of the keyword (see Table 7) A single layer LSTM along with a fully connected layer on top on the hidden state at last time step was used. Similar to experiments with

DeepSVDD, DeepSAD uses the hidden state of the final timestep as the representation in the one-class objective. An important aspect of training DeepSAD is the pretraining of the network as the encoder in an autoencoder. We also tuned this pretraining to ensure the best results.